JOURNAL OF GUIDANCE, CONTROL, AND DYNAMICS
Vol. 30, No. 4, July–August 2007

Pseudospectral Feedback Control for Three-Axis Magnetic Attitude Stabilization in Elliptic Orbits

Hui Yan*
Texas A&M University, College Station, Texas 77843
I. Michael Ross†
Naval Postgraduate School, Monterey, California 93943
and
Kyle T. Alfriend‡
Texas A&M University, College Station, Texas 77843

DOI: 10.2514/1.26591

In this paper a pseudospectral control law is applied to the magnetic attitude control of satellites in elliptic low Earth orbits. Our results show that three-axis magnetic attitude stabilization can be achieved by using a pseudospectral control law via the receding horizon control in elliptic orbits. The solutions from the pseudospectral control law are in excellent agreement with those obtained from the Riccati equation, but the computation speed improves by one order of magnitude. For the case investigated, the results show the effects of the known disturbing pitch torque are minimized when the satellite is in an unstable gravity gradient configuration.

Nomenclature

$\boldsymbol{B}$	=	Earth magnetic field
D	=	differentiation matrix
e	=	eccentricity
f	=	true anomaly
I_1, I_2, I_3	=	moments of inertia of the satellite about its principal axes, respectively
i	=	inclination
L_N	=	Legendre polynomial
$\boldsymbol{M}$	=	magnetic torque
$\boldsymbol{M_g}$	=	gravity gradient torque
$\boldsymbol{m}$	=	magnetic dipole vector, control variables in linear quadratic regulator
$\bar{\boldsymbol{m}}$	=	magnetic dipole vector, control variables in feedforward control loop
N	=	degree of Legendre polynomial
P_f	=	weight matrix for final states
$\hat{\boldsymbol{p}}$	=	Earth magnetic dipole unit vector
$Q(t)$	=	weight matrix for states
$\boldsymbol{R}$	=	position vector of the point at which the field is desired
$R_w(t)$	=	weight matrix for control variables
T_d	=	known disturbing pitch torque
T_f	=	magnetic torque in feedforward control
t	=	time since reference
u	=	argument of latitude
$\boldsymbol{X}$	=	state vector
θ	=	pitch angle
θ_{g0}	=	Greenwich sidereal time at some reference time
θ'_m	=	coelevation of the dipole
$\boldsymbol{\lambda}(t)$	=	costates
μ	=	gravitational parameter
μ_f	=	Earth magnetic field strength
ξ	=	Lagrange multiplier
τ_l	=	Legendre–Gauss–Lobatto points
ϕ	=	roll angle
ϕ'_m	=	East longitude of the dipole
ψ	=	yaw angle
Ω	=	longitude of the ascending node
ω_e	=	average rotation rate of the Earth
ω_0	=	orbital velocity
$\omega_1, \omega_2, \omega_3$	=	rotation rate of the body frame with respect to the inertial frame

I. Introduction

ATTITUDE stabilization is needed to maintain a spacecraft's attitude in the desired direction. In general, attitude stabilization systems are classified as active or passive. The simplicity and low cost of active magnetic control makes it an attractive option for small satellites in low Earth orbit (LEO) when precise attitude control is not a requirement.

There is a rich literature on active magnetic attitude stabilization [1–6]. Both linear and nonlinear methods have been investigated. For linearized magnetic attitude dynamic systems, linear quadratic regulators (LQR) have been considered for magnetic attitude stabilization [1,2,7]. A key challenge is the fact that the magnetic torque can only be produced in a plane perpendicular to the local Earth B-field vector, therefore the satellite is not controllable about the axis parallel to the field vector [1]. However, for orbits that are inclined to the Earth's magnetic equator, the direction of the field vector changes and it is possible to use this changing direction to stabilize motion over the entire orbit [5]. Solving the LQR problem for linear time-varying (LTV) systems requires an efficient computation of the Riccati equation, and solving Riccati equations in real time is CPU-intensive, particularly for legacy systems that continue to be used as onboard computers. To reduce this computational burden, steady-state periodic solutions obtained by averaging the periodic matrix in the Riccati equations have been proposed in [1,2]. The error caused by using the average is considered an additional external disturbance torque acting on the satellite.

In general, the operating orbits for Earth pointing satellites in LEO are restricted to near-circular orbits. However, there are some missions in which an elliptic orbit is desirable. Because the angular

Presented at the 16th AAS/AIAA Spaceflight Mechanics Meeting, Tampa, FL, 22–26 January 2006; received 17 July 2006; revision received 27 February 2007; accepted for publication 5 March 2007.

*Postdoctoral Associate, Department of Aerospace Engineering; hyan@tamu.edu. Senior Member AIAA

†Associate Professor, Department of Mechanical and Astronautical Engineering, Code ME/Ro; imross@nps.edu. Associate Fellow AIAA.

‡TEES Distinguished Research Chair Professor, Department of Aerospace Engineering; alfriend@aero.tamu.edu. Fellow AIAA.

velocity is time-varying in an elliptic orbit, there is a time-varying known disturbing pitch torque that is proportional to the eccentricity. Thus, to maintain the desired satellite attitude, which is usually nadir-pointing, some kind of passive or active control is required. As is well-known, the gravity gradient torque can be used to passively stabilize the attitude of a satellite. However, even if the gravity gradient torque stabilizes the spacecraft some active control may still be required. For this stabilization to be effective, the main requirement is a favorable inertia distribution. There are two stable inertia distributions for the case of a circular orbit. In the first case, a satellite's minor axis is vertical and the major axis is normal to the orbit. In this case the Hamiltonian is positive definite at the nadir-pointing equilibrium point; hence, it is Liapunov stable [8]. In the second case, the intermediate axis is aligned with the local vertical, and the minor axis is normal to the orbit. In this case the system is being stabilized by gyroscopic forces and the Hamiltonian is indefinite at the equilibrium point. Because the rotation is about the minor axis, any slight damping or disturbance will result in instability and drift away from the equilibrium point. Consequently, the second case is impractical for passive attitude control. In elliptic orbits, the known disturbing pitch torque due to the eccentricity can make a satellite tumble that would otherwise be stable in a circular orbit. The orbit eccentricity at which the satellite begins to tumble varies with the spacecraft shape, but is generally between 0.05 and 0.2 [9].

Active attitude stabilization in elliptic orbits was widely investigated in the 1960–70s [10–13]. The control methods focused on momentum exchange devices and cold gas plants. Magnetic attitude control has been used extensively since the 1970s for momentum bias LEO satellites [14,15]. Seldom were only magnetic torques proposed until the 1990s, when several papers appeared that proposed three-axis magnetic attitude stabilization for non-momentum bias satellites in circular orbits [1–5]. Each of these was for a small satellite.

One challenge of magnetic attitude stabilization is the specific direction of the magnetic torque, which is perpendicular to the Earth magnetic field. In elliptic orbits this is complicated by the presence of the known disturbing pitch torque that is periodic and its amplitude is proportional to the eccentricity. Because there will always be a component of this torque parallel to the magnetic filed torque, there is no way to totally reject the attitude librations due to the eccentricity using only magnetic torques.

In this paper we apply a pseudospectral control law for stabilizing the attitude of spacecraft in elliptic orbits. In recent years, pseudospectral methods have been used very effectively in solving a wide variety of nonlinear optimal control problems as illustrated in [16–18]. The basic idea of this method is to seek polynomial approximations for the state, costate, and control functions in terms of their values at the Legendre–Gauss–Lobatto (LGL) points. Thus it is apparent that LQR problems can be easily transformed into quadratic programming (QP) problems (a quadratic cost function subject to linear algebraic constraints) [19]. He and Unbehauen [20] compared pseudospectral techniques to Riccati methods in solving LQR problems and showed that there is a huge reduction in the number of equations to be solved, and the required computer memory storage. Although [19–22] solved their QP numerically, the analytical solutions were derived using preudospectral methods as shown in [23]. Compared with other analytical control laws that use step-by-step replacements for the states [24], this approach is quite easy to derive and implement.

Receding horizon control has become a useful and popular technique in implementing linear and nonlinear optimal control. In this technique an optimal control is determined online over a finite horizon in terms of the current time and states. The first move of the optimal control sequence is then implemented until the next measurements of the states are available. Repeating this procedure, the receding horizon technique generates a feedback control. The contribution of this paper is that we extend the analytical pseudospectral control law to the case including the known disturbing pitch torque caused by the eccentricity. Based on the extended analytical solutions, we propose a closed-form control law using a receding horizon control technique. Another important finding of the paper is that the unstable gravity gradient configuration is better than the stable gravity gradient configuration when minimizing the effect of disturbing gravity gradient torque in elliptic orbits using only magnetic torque. This is in sharp contrast with the case in circular orbits, where the stable gravity gradient configuration is preferred. Our results show that three-axis magnetic attitude stabilization is achieved by using the pseudospectral control law via the receding horizon control in elliptic orbits. The residual librations errors are within 1 deg for an eccentricity of 0.1.

II. Coordinate Frame

A. Inertial Frame

The X_e axis points to the vernal point in the equatorial plane of the Earth. The Z_e axis is the axis of rotation of the Earth in a positive direction and Y_e is defined by the right-hand rule.

B. Magnetic Equator Frame

Assume the x_m axis is along the line of nodes between the magnetic equator plane and orbit plane, the z_m axis is perpendicular to the magnetic equator plane and points toward the northern hemisphere of the Earth, and y_m is defined by the right-hand rule.

C. Orbit Frame

The origin is attached to the spacecraft. The z axis points from the spacecraft to the Earth center, the y axis follows the negative normal direction the orbit plane and the x axis is defined by the right-hand rule and points approximately along the velocity vector. We use this frame as the reference frame in spacecraft attitude control.

D. Body Frame

The attitude coordinates are chosen to be the (3-2-1) Euler angles: roll angle ϕ about x_1 axis, pitch angle θ about y_1 axis, and yaw angle ψ about z_1 axis under small Euler angle assumptions. The x_1, y_1, and z_1 axes align with the principal body axes, and the body frame coincides with the orbit frame when the Euler angles are zeros.

III. Earth Magnetic Field Model

From [25], the magnetic field approximated by a dipole model is

$$\boldsymbol{B} = \frac{\mu_f}{R^3}[3(\hat{\boldsymbol{p}} \cdot \hat{\boldsymbol{R}})\hat{\boldsymbol{R}} - \hat{\boldsymbol{P}}] \tag{1}$$

The field's dipole strength is $\mu_f = 7.9 \times 10^{15}$ (Wb · m) and in the inertial frame

$$\hat{\boldsymbol{p}} = \begin{bmatrix} \sin\theta'_m \cos\alpha_m \\ \sin\theta'_m \sin\alpha_m \\ \cos\theta'_m \end{bmatrix} \tag{2}$$

where

$$\alpha_m = \theta_{g0} + \omega_e t + \phi'_m \tag{3}$$

Here we express the Earth magnetic field in the orbit frame and consider the Earth rotation. The transformation matrix from the inertial frame to the orbit frame is

$$R_{OE} = \begin{bmatrix} -\sin u\cos\Omega - \cos u\cos i\sin\Omega & -\sin u\sin\Omega + \cos u\cos i\cos\Omega & \cos u\sin i \\ -\sin i\sin\Omega & \sin i\cos\Omega & -\cos i \\ -\cos u\cos\Omega + \sin u\cos i\sin\Omega & -\cos u\sin\Omega - \sin u\cos i\cos\Omega & -\sin u\sin i \end{bmatrix} \tag{4}$$

In the orbit frame the expression of the rotating Earth magnetic field is

$$\boldsymbol{B} = \frac{\mu_f}{R^3} R_{OE}[3(\hat{\boldsymbol{p}} \cdot \hat{\boldsymbol{R}})\hat{\boldsymbol{R}} - \hat{\boldsymbol{P}}] \tag{5}$$

IV. Magnetic Attitude Dynamic Model

The angular equations of motion are

$$\dot{\omega}_1 = \frac{M_1 + M_{g1}}{I_1} + \frac{I_2 - I_3}{I_1}\omega_2\omega_3 \tag{6}$$

$$\dot{\omega}_2 = \frac{M_2 + M_{g2}}{I_2} + \frac{I_3 - I_1}{I_2}\omega_1\omega_3 \tag{7}$$

$$\dot{\omega}_3 = \frac{M_3 + M_{g3}}{I_3} + \frac{I_1 - I_2}{I_3}\omega_1\omega_2 \tag{8}$$

The applied magnetic moments are

$$\boldsymbol{M} = \boldsymbol{m} \times \boldsymbol{B} \tag{9}$$

where the control variables $\boldsymbol{m}$ are the magnetic dipole moments of the torque rods and magnetic torque $\boldsymbol{M} = [M_1 \quad M_2 \quad M_3]^T$. The gravity gradient moments are [26]

$$\boldsymbol{M}_g = 1.5\frac{\mu}{R^3}\begin{pmatrix} (I_3 - I_2)\cos^2\theta \sin 2\phi \\ -(I_1 - I_3)\cos\phi \sin 2\theta \\ -(I_2 - I_1)\sin\phi \sin 2\theta \end{pmatrix} \tag{10}$$

and $\boldsymbol{M}_g = [M_{g1} \quad M_{g2} \quad M_{g3}]^T$.

The body angular velocity relative to the orbit frame expressed in the body frame is

$$\boldsymbol{\omega}_{B/O} = \begin{bmatrix} -\sin\theta & 0 & 1 \\ \sin\phi\cos\theta & \cos\phi & 0 \\ \cos\phi\cos\theta & -\sin\phi & 0 \end{bmatrix}\begin{bmatrix} \dot{\psi} \\ \dot{\theta} \\ \dot{\phi} \end{bmatrix} \tag{11}$$

We have

$$\boldsymbol{\omega}_{B/E} = \boldsymbol{\omega}_{B/O} + \boldsymbol{R}_{BO}\begin{bmatrix} 0 \\ -\boldsymbol{\omega}_0 \\ 0 \end{bmatrix} \tag{12}$$

The transformation matrix is

$$\boldsymbol{R}_{BO} = \begin{bmatrix} \cos\theta\cos\psi & \cos\theta\sin\psi & -\sin\theta \\ \sin\phi\sin\theta\cos\psi - \cos\phi\sin\psi & \sin\phi\sin\theta\sin\psi + \cos\phi\cos\psi & \sin\phi\cos\theta \\ \cos\phi\sin\theta\cos\psi + \sin\phi\sin\psi & \cos\phi\sin\theta\sin\psi - \sin\phi\cos\psi & \cos\phi\cos\theta \end{bmatrix} \tag{13}$$

Linearizing for small angles and rates and substituting gives

$$\dot{\boldsymbol{X}} = A\boldsymbol{X} + G\boldsymbol{m} + \boldsymbol{F}_d \tag{14}$$

$$\boldsymbol{X} = [\phi \quad \theta \quad \psi \quad \dot{\phi} \quad \dot{\theta} \quad \dot{\psi}]^T \tag{15}$$

where

$$\boldsymbol{F}_d = [0 \quad 0 \quad 0 \quad 0 \quad \dot{\omega}_0 \quad 0]^T \tag{16}$$

$$A = \begin{bmatrix} 0 & 0 & 0 & 1 & 0 & 0 \\ 0 & 0 & 0 & 0 & 1 & 0 \\ 0 & 0 & 0 & 0 & 0 & 1 \\ -\left(3\frac{\mu}{R^3} + \omega_0^2\right)\sigma_1 & 0 & \dot{\omega}_0 & 0 & 0 & \omega_0(1-\sigma_1) \\ 0 & 3\frac{\mu}{R^3}\sigma_2 & 0 & 0 & 0 & 0 \\ -\dot{\omega}_0 & 0 & \omega_0^2\sigma_3 & -\omega_0(1+\sigma_3) & 0 & 0 \end{bmatrix} \tag{17}$$

$$G = \begin{bmatrix} 0 & 0 & 0 \\ 0 & 0 & 0 \\ 0 & 0 & 0 \\ 0 & \frac{B_3}{I_1} & -\frac{B_2}{I_1} \\ -\frac{B_3}{I_2} & 0 & \frac{B_1}{I_2} \\ \frac{B_2}{I_3} & -\frac{B_1}{I_3} & 0 \end{bmatrix} \tag{18}$$

$$\boldsymbol{m} = [m_1 \quad m_2 \quad m_3]^T \tag{19}$$

$$\boldsymbol{B} = [B_1 \quad B_2 \quad B_3]^T \tag{20}$$

$$\sigma_1 = (I_2 - I_3)/I_1, \qquad \sigma_2 = (I_3 - I_1)/I_2, \qquad \sigma_3 = (I_1 - I_2)/I_3 \tag{21}$$

V. Control Law Design

There is a forcing term in Eq. (14). The angular velocity can be expressed as

$$\dot{\omega} = -2e\mu \sin f/R^3 \tag{22}$$

Assume

$$K = -2I_2 e\mu/R^3 \tag{23}$$

then the forcing term

$$T_d = I_2\dot{\omega}_0 = K \sin f \tag{24}$$

T_d is the known disturbing pitch torque. A standard way of minimizing the effect of a known disturbance is to feed forward the estimate of the torque to the control system so that the system does not have to wait to respond to the effect of the torque. Because feedforward is open-loop control, an LQR is used coincidently together with the feedforward control to compensate for the latter's inaccuracies and track reference trajectories.

A. Feedforward Control Design

Magnetic torques are used to reject the known disturbing pitch torque. The magnetic control torques are

$$T_{f1} = \bar{m}_2 B_3 - \bar{m}_3 B_2 \tag{25}$$

$$T_{f2} = \bar{m}_3 B_1 - \bar{m}_1 B_3 \tag{26}$$

$$T_{f3} = \bar{m}_1 B_2 - \bar{m}_2 B_1 \tag{27}$$

where $\bar{m}_1$, $\bar{m}_2$, $\bar{m}_3$ are the components of the dipole vector $\bar{\boldsymbol{m}}$ in the body frame. Because the known disturbing pitch torque is along the pitch direction, Eqs. (25–27) indicate we cannot totally reject the disturbance due to magnetic interaction. To minimize the known disturbing pitch torque effects, we introduce the following performance index:

$$J_f = T_{f1}^2 + (T_{f2} - T_d)^2 + T_{f3}^2 \tag{28}$$

The magnetic control torque is

$$\boldsymbol{T}_f = \bar{\boldsymbol{m}} \times \boldsymbol{B} \tag{29}$$

One can see from Eq. (29) that the minimum $\|\bar{\boldsymbol{m}}\|$ occurs when [27]

$$\bar{\boldsymbol{m}} \cdot \boldsymbol{B} = 0 \tag{30}$$

because a magnetic moment generated in the direction parallel to the magnetic field has no influence on the attitude control. The augmented performance after adding Eq. (30) to Eq. (28) and substituting for the control torques gives

$$\bar{J}_f = (\bar{m}_2 B_3 - \bar{m}_3 B_2)^2 + (\bar{m}_3 B_1 - \bar{m}_1 B_3 - K \sin f)^2 + (\bar{m}_1 B_2 - \bar{m}_2 B_1)^2 + \xi \bar{\boldsymbol{m}} \cdot \boldsymbol{B} \tag{31}$$

where ξ is a Lagrange multiplier. Taking the partials for the optimal solution gives

$$\bar{m}_1 = -\frac{B_3}{B^2} K \sin f \tag{32}$$

$$\bar{m}_2 = 0 \tag{33}$$

$$\bar{m}_3 = \frac{B_1}{B^2} K \sin f \tag{34}$$

where $B^2 = B_1^2 + B_2^2 + B_3^2$. Substituting Eqs. (32–34) into Eq. (28), we have

$$J_f = \frac{B_2^2}{B^2} (K \sin f)^2 \tag{35}$$

which is much less than one without feedforward control.

B. LQR Control Design

Considering the feedforward control term, Eq. (14) becomes

$$\dot{\boldsymbol{X}} = A\boldsymbol{X} + G(\boldsymbol{m} - \bar{\boldsymbol{m}}) + \boldsymbol{F}_d \tag{36}$$

with the initial conditions

$$\boldsymbol{X}(t_0) = \boldsymbol{X}_0 \tag{37}$$

The problem is to determine the optimal control $\boldsymbol{m}(t)$ and corresponding state vector $\boldsymbol{X}(t)$ satisfying Eqs. (36) and (37) while minimizing

$$J = \frac{1}{2} \boldsymbol{X}^T(t_f) P_f \boldsymbol{X}(t_f) + \frac{1}{2} \int_{t_0}^{t_f} [\boldsymbol{X}^T(t) Q(t) \boldsymbol{X}(t) + \boldsymbol{m}^T(t) R_w(t) \boldsymbol{m}(t)] \, \mathrm{d}t \tag{38}$$

The Hamiltonian for this system is

$$H = \frac{1}{2} [\boldsymbol{X}^T(t) Q(t) \boldsymbol{X}(t) + \boldsymbol{m}^T(t) R_w(t) \boldsymbol{m}(t)] + \boldsymbol{\lambda}^T(t)(A\boldsymbol{X} + G\boldsymbol{m} - G\bar{\boldsymbol{m}} + \boldsymbol{F}_d) \tag{39}$$

According to Pontryagin's Minimum Principle, we have the costate equations

$$\dot{\boldsymbol{\lambda}}(t) = -\frac{\partial H}{\partial \boldsymbol{X}} = -[Q(t)\boldsymbol{X}(t) + A^T(t)\boldsymbol{\lambda}(t)] \tag{40}$$

and the necessary optimality conditions

$$\frac{\partial H}{\partial \boldsymbol{m}} = 0 \quad \text{or} \quad \boldsymbol{m}(t) = F(t)\boldsymbol{\lambda}(t) \tag{41}$$

where $F(t) = -R_w^{-1}(t) G^T(t)$

The transversality conditions are

$$\boldsymbol{\lambda}(t_f) = P_f \boldsymbol{X}(t_f) \tag{42}$$

Substituting Eq. (41) into Eq. (36), we have the following linear two-point boundary value problem (TPBVP) :

$$\begin{bmatrix} \dot{\boldsymbol{X}} \\ \dot{\boldsymbol{\lambda}} \end{bmatrix} = \begin{bmatrix} A(t) & G(t)F(t) \\ -Q(t) & -A^T(t) \end{bmatrix} \begin{bmatrix} \boldsymbol{X} \\ \boldsymbol{\lambda} \end{bmatrix} + \begin{bmatrix} -G(t)\bar{\boldsymbol{m}} + \boldsymbol{F}_d \\ \boldsymbol{O}_n \end{bmatrix} \tag{43}$$

where $\boldsymbol{O}_n$ is a $n \times 1$ zero vector. Analytical control laws will be obtained with the Legendre pseudospectral method by solving Eq. (43) with the conditions Eqs. (37) and (42).

VI. Pseudospectral Method

The basic idea of this method is to seek polynomial approximations for the state, costate, and control functions in terms of their values at the LGL points. Then the LTV system with quadratic criteria is reduced to solving a system of algebraic equations. Based on the algebraic equations, analytical control laws can be derived.

Because the problem presented in the preceding section is formulated over the time interval $[t_0.t_f]$, and the LGL points lie in the interval $[-1, 1]$, we use the following transformation to express the problem for $\tau \in [\tau_0, \tau_N] = [-1, 1]$:

$$t = \frac{(t_f - t_0)\tau + (t_f + t_0)}{2} \tag{44}$$

The use of the symbol τ_N (which maps to t_f) will be apparent shortly. It follows that Eqs. (37), (42), and (43) can be replaced by

$$\dot{\boldsymbol{X}}(\tau) = \frac{t_f - t_0}{2} [A(\tau)\boldsymbol{X}(\tau) + G(\tau)F(\tau)\boldsymbol{\lambda}(\tau) - G(\tau)\bar{\boldsymbol{m}} + \boldsymbol{F}_d] \tag{45}$$

$$\dot{\boldsymbol{\lambda}}(\tau) = -\frac{t_f - t_0}{2} [Q(\tau)\boldsymbol{X}(\tau) + A^T(\tau)\boldsymbol{\lambda}(\tau)] \tag{46}$$

$$\boldsymbol{X}(-1) = \boldsymbol{X}_0 \tag{47}$$

$$\boldsymbol{\lambda}(1) = S\boldsymbol{X}(1) \tag{48}$$

Let $L_N(\tau)$ be the Legendre polynomial of degree N on the interval $[-1, 1]$. In the Legendre pseudospectral approximation of Eqs. (45–48), we use the LGL points, τ_l, $l = 0, \ldots, N$, which are given by

$$\tau_0 = -1, \qquad \tau_N = 1 \tag{49}$$

and for $1 \le l \le N - 1$, τ_1 are the zeros of $\dot{L}_N$, the derivative of the Legendre polynomial L_N. There are no closed-form expressions for these nodes, and they have to be computed numerically. For approximating the continuous equations, we seek a polynomial approximation of the form

$$X^N(\tau) = \sum_{l=0}^{N} X(\tau_l)\phi_l(\tau) \tag{50}$$

$$m^N(\tau) = \sum_{l=0}^{N} m(\tau_1)\phi_l(\tau) \tag{51}$$

$$\lambda^N(\tau) = \sum_{l=0}^{N} \lambda(\tau_l)\phi_l(\tau) \tag{52}$$

where for $l = 0, 1, \ldots, N$

$$\phi_l(\tau) = \frac{1}{N(N+1)L_N(\tau_l)} \frac{(\tau^2 - 1)\dot{L}_N(\tau)}{\tau - \tau_l} \tag{53}$$

are the Lagrange polynomials of order N. Notice the superscript N does not mean the power of the variables. It can be shown that

$$\phi_l(\tau_k) = \delta_{lk} = \begin{cases} 1 & \text{if } l = k \\ 0 & \text{if } l \neq k \end{cases} \tag{54}$$

From this property of ϕ_l it follows that

$$\boldsymbol{X}^N(\tau_l) = \boldsymbol{X}(\tau_l), \qquad \boldsymbol{m}^N(\tau_l) = \boldsymbol{m}(\tau_l), \qquad \boldsymbol{\lambda}^N(\tau_l) = \boldsymbol{\lambda}(\tau_l) \tag{55}$$

To express the derivatives $\dot{\boldsymbol{X}}^N$ and $\dot{\boldsymbol{\lambda}}^N$ in terms of $\boldsymbol{X}^N(\tau)$ and $\boldsymbol{\lambda}^N(\tau)$ at the collocation points τ_l, respectively, we differentiate Eqs. (50) and (52), which results in a matrix multiplication of the following forms:

$$\dot{\boldsymbol{X}}^N(\tau_k) = \sum_{l=0}^{N} D_{kl}\boldsymbol{X}(\tau_l) \tag{56}$$

$$\dot{\boldsymbol{\lambda}}^N(\tau_k) = \sum_{l=0}^{N} D_{kl}\boldsymbol{\lambda}(\tau_l) \tag{57}$$

where the D_{kl} are the entries of the $(N+1) \times (N+1)$ differentiation matrix D:

$$D = [D_{kl}] = \begin{cases} \frac{L_N(\tau_k)}{L_N(\tau_l)} \frac{1}{\tau_k - \tau_l} & k \neq l \\ -\frac{N(N+1)}{4} & k = l = 0 \\ \frac{N(N+1)}{4} & k = l = N \\ 0 & \text{otherwise} \end{cases} \tag{58}$$

Setting

$$\boldsymbol{a} = (\boldsymbol{a}_0^T, \boldsymbol{a}_1^T, \ldots, \boldsymbol{a}_N^T)^T \tag{59}$$

$$\boldsymbol{b} = (\boldsymbol{b}_0^T, \boldsymbol{b}_1^T, \ldots, \boldsymbol{b}_N^T)^T \tag{60}$$

$$\boldsymbol{c} = (\boldsymbol{c}_0^T, \boldsymbol{c}_1^T, \ldots, \boldsymbol{c}_N^T)^T \tag{61}$$

we use the notation

$$\boldsymbol{a}_l := \boldsymbol{X}(\tau_l), \qquad \boldsymbol{b}_l := \boldsymbol{m}(\tau_l), \qquad \boldsymbol{c}_l := \boldsymbol{\lambda}(\tau_l) \tag{62}$$

to rewrite Eqs. (50–52) in the form

$$\boldsymbol{X}^N(\tau) = \sum_{l=0}^{N} \boldsymbol{a}_l\phi_l(\tau) \tag{63}$$

$$\boldsymbol{m}^N(\tau) = \sum_{l=0}^{N} \boldsymbol{b}_l\phi_l(\tau) \tag{64}$$

$$\boldsymbol{\lambda}^N(\tau) = \sum_{l=0}^{N} \boldsymbol{c}_l\phi_l(\tau) \tag{65}$$

Equations (45) and (46) and Eq. (41) are discretized and transformed into the following algebraic equations in terms of the coefficients a, b, and c at the LGL nodes, t_k:

$$\sum_{l=0}^{N} D_{kl}\boldsymbol{a}_l - \frac{\tau_f - \tau_0}{2}(A_k\boldsymbol{a}_k + G_kF_k\boldsymbol{c}_k) = \frac{\tau_f - \tau_0}{2}(\boldsymbol{F}_{dk} - G_k\bar{\boldsymbol{m}}_k) \tag{66}$$

$$\sum_{l=0}^{N} D_{kl}\boldsymbol{c}_l + \frac{\tau_f - \tau_0}{2}\left(Q_k\boldsymbol{a}_k + A_k^T\boldsymbol{c}_k\right) = 0 \tag{67}$$

$$\boldsymbol{b}_k - F_k\boldsymbol{c}_k = 0 \qquad k = 0, 1, \ldots, N \tag{68}$$

or

$$\tilde{A}_-\boldsymbol{a} - \frac{\tau_f - \tau_0}{2}\tilde{G}\boldsymbol{c} = \boldsymbol{V}_f \tag{69}$$

$$\frac{\tau_f - \tau_0}{2}\tilde{Q}\boldsymbol{a} + \tilde{A}_+\boldsymbol{c} = 0 \tag{70}$$

$$\boldsymbol{b} - P\boldsymbol{c} = 0 \tag{71}$$

where $\tilde{A}_-$, $\tilde{A}_+$, $\tilde{G}$, $\tilde{Q}$, and P are $[n \times (N+1)] \times [n \times (N+1)]$ matrices whose ijth blocks are $n \times n$ matrices of the following form:

$$[\tilde{A}_-]_{ij} = \begin{cases} D_{ij}I_n & i \neq j \\ D_{ii}I_n - \frac{\tau_f - \tau_0}{2}A_i & i = j \end{cases} \tag{72}$$

$$[\tilde{A}_+]_{ij} = \begin{cases} D_{ij}I_n & i \neq j \\ D_{ii}I_n + \frac{\tau_f - \tau_0}{2}A_i^T & i = j \end{cases} \tag{73}$$

$$[\tilde{G}]_{ij} = \begin{cases} 0_n & i \neq j \\ \bar{B}_iF_i & i = j \end{cases} \tag{74}$$

$$[\tilde{Q}]_{ij} = \begin{cases} 0_n & i \neq j \\ Q_i & i = j \end{cases} \tag{75}$$

$$[P]_{ij} = \begin{cases} 0_n & i \neq j \\ F_i & i = j \end{cases} \tag{76}$$

In the preceding equations, I_n is a $n \times n$ unity matrix and 0_n is a $n \times n$ zero matrix. $\boldsymbol{V}_f$ is a vector and

$$[\boldsymbol{V}_f]_i = \frac{\tau_f - \tau_0}{2}(\boldsymbol{F}_{di} - G_i\bar{\boldsymbol{m}}_i) \tag{77}$$

The initial conditions are

$$\boldsymbol{a}(0) = \boldsymbol{a}_0 \tag{78}$$

For unconstrained linear systems, the stability of receding horizon control is established by forcing the terminal constraints [28,29],

$$\boldsymbol{a}(N) = 0 \tag{79}$$

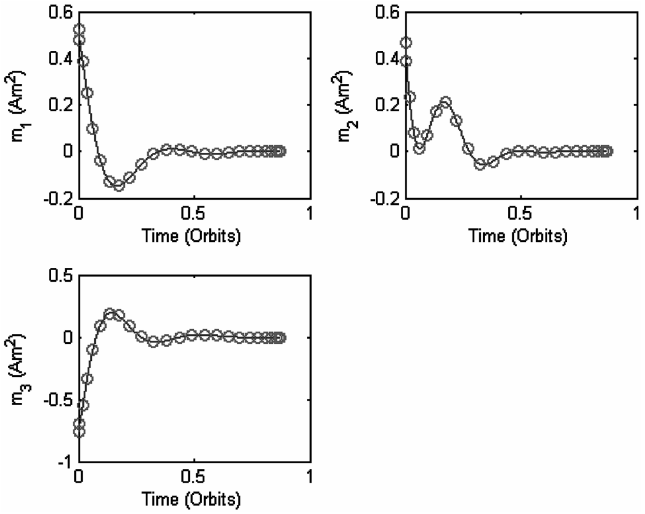

Fig. 1 Magnetic dipole moment: pseudospectral control law vs Riccati solutions.

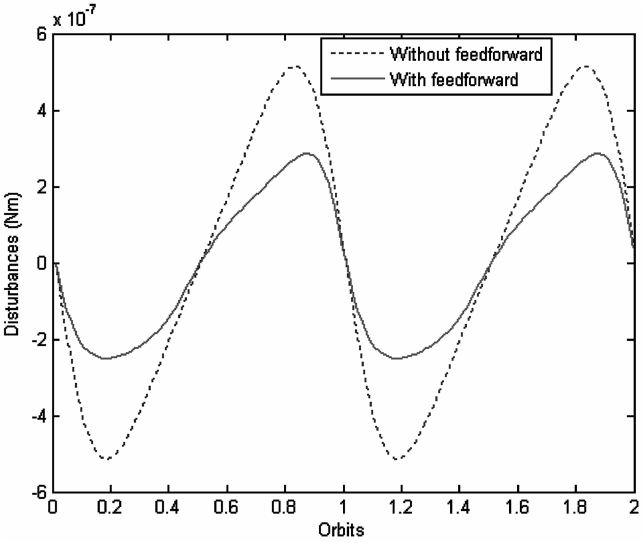

Fig. 2 Disturbance comparison.

$$\boldsymbol{c}(N) = 0 \tag{80}$$

to convert an infinite horizon, open-loop optimal control problem to a finite horizon problem. In [30], it can be shown, under a practically verifiable condition, a sequence of pseudospectral discrete optimal solutions converges to the optimal solution of the original continuous problem.

The goal is to solve the linear equation, Eqs. (61–71), subject to the transversality conditions Eqs. (78–80). The procedure to derive an analytical feedback control law is the same as one in [23], except that we introduce the known disturbing pitch torque F_d and feedforward control into the linear equation Eq. (36). Please see [31] for the complete derivation.

VII. Simulation Results

We consider NPSAT1, a magnetically controlled small satellite [7]. There are three rods, one along each axis in the satellite. Table 1 lists the simulation parameters.

A. Pseudospectral vs Riccati Solutions

Here we take a 560 km altitude circular orbit as an example. Assume the initial Euler angles errors are about 30 deg and angular velocities are 0.03 deg/s on all three axes. Obtaining control laws using the Riccati equation involves 1) integrating the Riccati equation backward in time, 2) storing this solution, and then 3) integrating the state equations in forward.

Figure 1 shows comparisons between the pseudospectral solutions and the Riccati solutions. In the figure, the solid lines represent the solutions from the Riccati equation, whereas the circles stand for those from the pseudospectral control law. The number of LGL points used is 30. From this figure one can see that the comparison between the pseudospectral and Riccati solutions is excellent. The computation time for the pseudospectral control law is about 0.3 s, whereas obtaining the control law from the Riccati solutions takes about 4 s. There is one order of magnitude improvement in the computation time using the pseudospectral control law and the results are the same as those from the Riccati equations. In Table 1 the saturation is 30 Am^2 for the magnetic dipole moments of the torque rods. Here one can see actual optimal dipole moments are far less than this saturation, as shown in Fig. 1.

Table 1 Simulation parameters

Parameter and units	Value
Eccentricity	0.1
Semimajor axis, km	560
Inclination, deg	35.4
Inertia, $\text{kg} \cdot \text{m}^2$	5.1, 5, 2
Magnetic torque rod saturation, $\text{A} \cdot \text{m}^2$	30

The elliptic orbit introduces parametric excitations and forcing terms not present in circular orbits. As shown in [32], the initial conditions have negligible effect on the long-term behavior of the solutions, the terms due to the initial perturbations will tend to zero and the solution approaches the forced response as time increases.

B. Magnetic Attitude Control in Elliptic Orbits

1. *Feedforward Control*

The known disturbing pitch torque can be found in Eq. (24). The remaining torque can be seen in Eq. (35) after using the feedforward control. Figure 2 shows that the remaining torque is much less than the known disturbing pitch torque.

2. *Pseudospectral Control Law via Receding Horizon Control Implementation*

Choose 30 LGL points. The horizon is selected as one orbit period. Starting at the initial time, we take the sampling for the current states every 50 s. The total samples are 1000. Once the control law is obtained with the initial conditions over the given horizon, the actual trajectory is then computed with the nonlinear dynamics governed by the system Eqs. (6–8), (11), and (12) plus the feedforward control. The next state conditions $\delta \boldsymbol{X}$ are generated from $\delta \boldsymbol{X} = \boldsymbol{X} - \boldsymbol{X}^*$, where $\boldsymbol{X}$ is the state response from system Eqs. (6–8), (11), and (12) and the asterisk denotes the reference value which should be zero for stabilizations. In other words, the $\delta \boldsymbol{X}$ are the actual values, not those generated from the linear equations, Eqs. (36). Repeat this procedure to form the receding horizon control.

Assume all the initial conditions are zeros. Consider the following inertia distributions:

$$\text{Case 1: } I_2 > I_1 > I_3 \qquad \text{Case 2: } I_1 > I_3 > I_2$$

In case 1, $I_1 = 5\ \text{kg} \cdot \text{m}^2$, $I_2 = 5.1\ \text{kg} \cdot \text{m}^2$, $I_3 = 2\ \text{kg} \cdot \text{m}^2$, whereas in case 2, $I_1 = 5.1\ \text{kg} \cdot \text{m}^2$, $I_2 = 2\ \text{kg} \cdot \text{m}^2$, $I_3 = 5\ \text{kg} \cdot \text{m}^2$. Figures 3–6 show the magnetic control and Euler angle time histories for the two cases.

Case 1 represents static stabilization whereas case 2 is statically unstable [8]. The stable gravity gradient attitude system works better than the unstable system in the circular orbit. However, comparing Fig. 4 with Fig. 6, the Euler angles in case 2 are much smaller than those in case 1. A comparison of Figs. 3 and 5 shows that the magnetic control effort is also less in case 2. This result is caused by the different disturbance angular accelerations due to different inertia ratios as the unstable gravity gradient torque is smaller in the forced

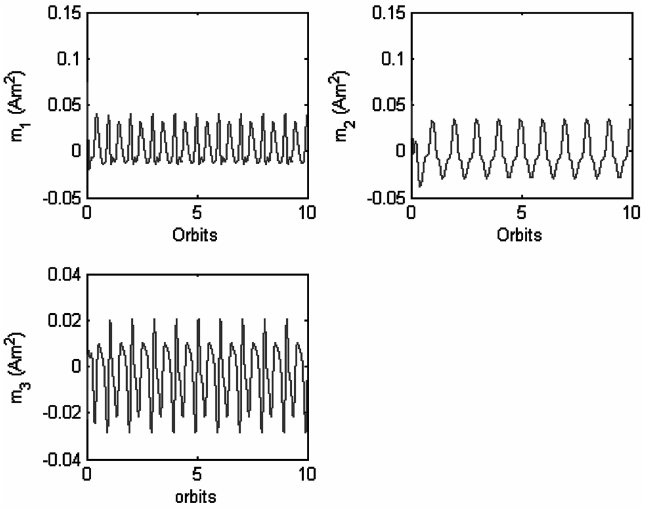

Fig. 3 Case 1: magnetic dipole moments.

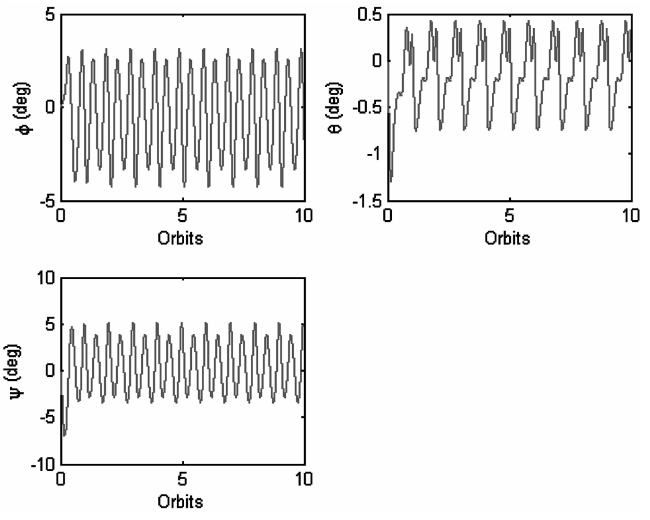

Fig. 4 Case 1: Euler angles.

steady state. Substituting Eqs. (32–34) into Eqs. (25–27), the disturbance angular accelerations in the roll, pitch, and yaw axes are

$$a_{d1} = -2ek_1\left(\frac{B_1B_2}{B^2}\right)\left(\frac{\mu}{R^3}\right)\sin f \tag{81}$$

$$a_{d2} = -2e\left(\frac{B_2^2}{B^2}\right)\left(\frac{\mu}{R^3}\right)\sin f \tag{82}$$

$$a_{d3} = -2ek_3\left(\frac{B_2B_3}{B^2}\right)\left(\frac{\mu}{R^3}\right)\sin f \tag{83}$$

where

$$k_1 = \frac{I_2}{I_1} \qquad k_3 = \frac{I_2}{I_3} \tag{84}$$

From Eqs. (81–84), one can see there is a big difference in the disturbance angular accelerations due to the different inertia ratios for cases 1 and 2. For example, $k_3 = 2.55$ in case 1 whereas $k_3 = 0.4$ in case 2, which means the disturbance acceleration of case 1 is 6.4 times more than that of case 2 in the yaw axis and 2.6 times in the roll axis.

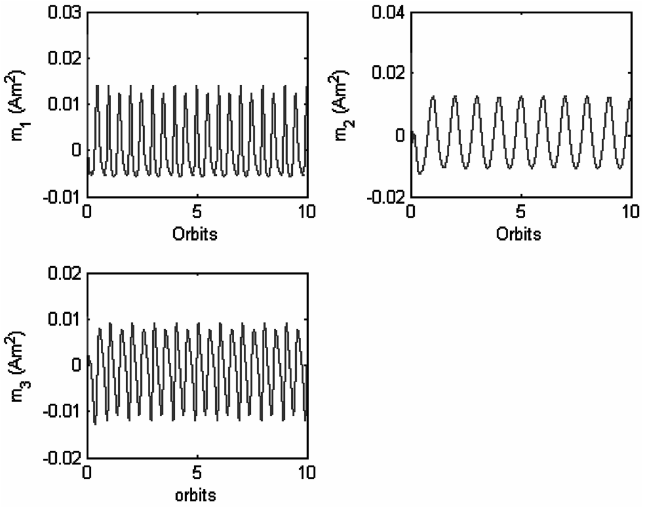

Fig. 5 Case 2: magnetic dipole moments.

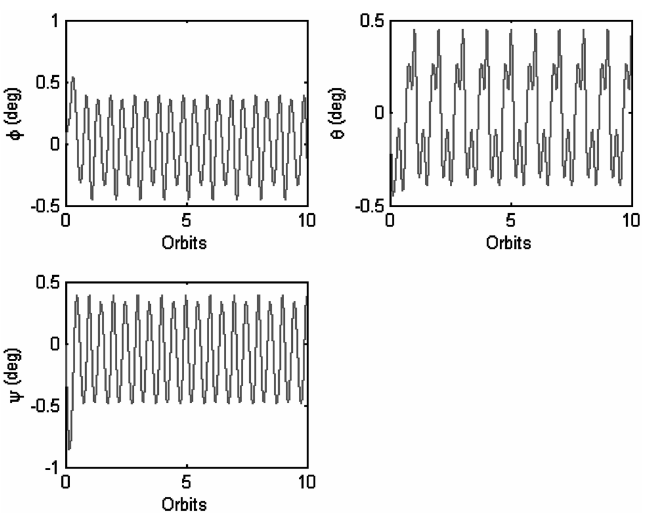

Fig. 6 Case 2: Euler angles.

3. Effects of Inertia Distributions

As we observe the inertia distributions have a significant effect on the performance of the magnetic attitude control system. Figure 7 illustrates the simulation results from random inertia distribution samples. In the figure the circles represent the solutions where the maximum Euler angles are less than 1 deg at the final stage. The stars stand for the ones where the maximum Euler angles are over 1 deg.

From Fig. 7 one can see most of the solutions satisfy the 1-deg accuracy requirement if k_1 and k_3 are less than 0.5. Another possible choice is k_1 or k_3 less than 0.2. Figure 7 shows that in this case the effects of the known disturbing pitch torque are minimized when the maximum inertia matrix is either the roll or yaw axis.

4. Initial Perturbations Effects

Assume the initial Euler angles errors are about 30 deg and the angular velocities are zero on all three axes. The simulations were performed using the nonlinear dynamic model input with the pseudospectral control laws. The results show that the pseudospectral control law works well for magnetic attitude stabilization in elliptic orbits. Figures 8 and 9 show Euler angles time histories for cases 1 and 2.

The initial errors are rejected and the attitude is stabilized in less than one orbit period, as shown in Figs. 8 and 9. The transient responses demonstrate good performance and fast decays with one or two oscillations about the equilibrium where the magnetic torques and the known disturbing pitch torques balance. The transient

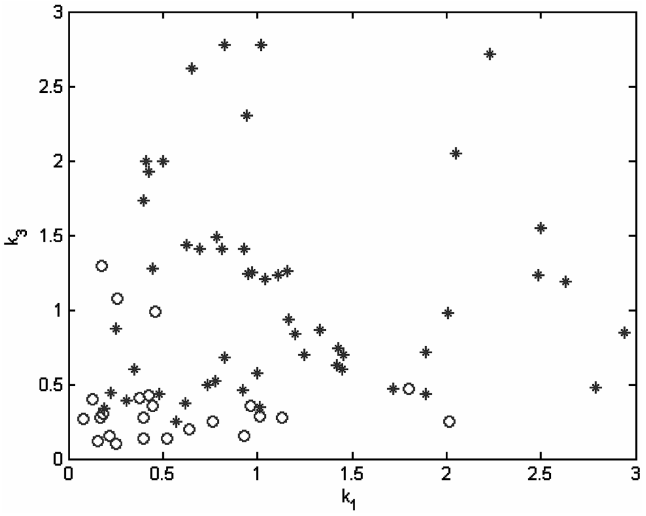

Fig. 7 Effects of inertia distributions.

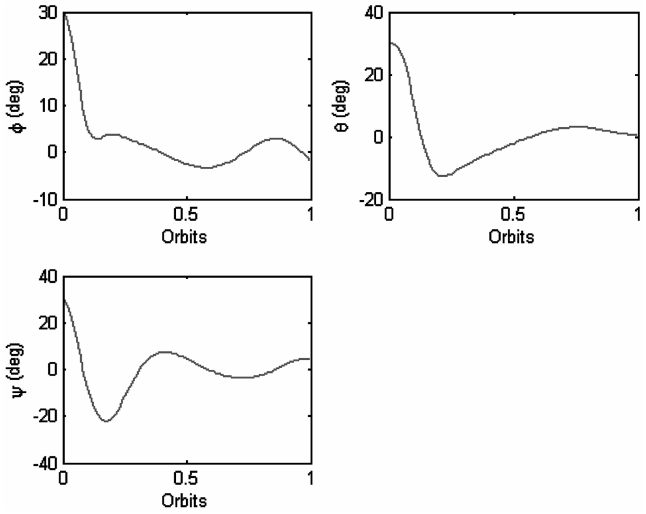

Fig. 8 Euler angles (Case 1).

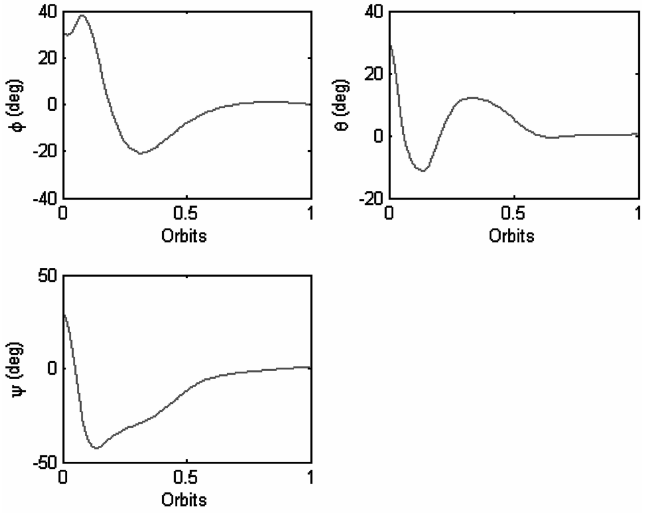

Fig. 9 Euler angles (Case 2).

responses of case 1 are much better than that of case 2 as result of the stable gravity gradient torque in case 1. In the initial phase the gravity gradient torque plays a major rule and dominates the known disturbing pitch torque. As the initial large angle error is nullified, the gravity gradient torque becomes small and the primary torque is the known disturbing pitch torque that is proportional to eccentricity. For the best magnetic attitude control in elliptic orbits, we suggest favorable inertial distributions should be static gravity gradient stabilization in the initial phase, then satellites make 90 deg fast slew maneuver as illustrated in [33], having the roll or yaw axis as the maximum inertia minimizes the angular disturbance accelerations caused by the eccentricity in steady phase.

VIII. Conclusions

Three-axis magnetic attitude stabilization for satellites in elliptic low Earth orbits can be achieved by using a pseudospectral control law via the receding horizon technique. The solutions from the pseudospectral control law are in excellent agreement with those obtained from the Riccati equation, but the computation speed improves by one order of magnitude. The control law indicates the solutions consist of natural and forced responses. The known disturbing pitch torque is greatly rejected by using a feedforward control. Numerical solutions show that natural responses quickly tend to the region where the attitude motion is steady state, even with large initial angle errors. For the case investigated, an interesting result occurs in that the effect of the known disturbing pitch torque, which is proportional to the eccentricity, is minimized when the satellite is an unstable gravity gradient configuration, that is, the maximum inertia is along the yaw or roll axis.

References

[1] Wisniewski, R., "Linear Time Varying Approach to Satellite Attitude Control Using Only Electromagnetic Actuation," *Proceedings of the AIAA Guidance, Navigation, and Control Conference*, Vol. 23, AIAA, Reston, VA, 1997, pp. 243–251.

[2] Psiaki, M. L., "Magnetic Torquer Attitude Control via Asymptotic Periodic Linear Quadratic Regulation," *Journal of Guidance, Control, and Dynamics*, Vol. 24, No. 2, 2001, pp. 386–394.

[3] Wang, P., and Shtessel, Y. B., "Satellite Attitude Control Using Only Magnetic Torquers," *Proceedings of the AIAA Guidance, Navigation, and Control Conference*, Vol. 23, AIAA, Reston, VA, 1998, pp. 1490–1498.

[4] Martel, F., Pal, P. K., and Psiaki, M. L., "Active Magnetic Control System for Gravity Gradient Stabilized Spacecraft," *Proceedings of the 2nd Annual AIAA/USU Conference on Small Satellites*, Small Satellite Conference Services, Utah State Univ., Logan, UT, 1988, pp. 1–19.

[5] Kulkarni, J., and Campbell, M., "An Approach to Magnetic Torque Attitude Control of Satellites via 'H_∞' Control for LTV Systems," *Proceedings of the 43rd IEEE Conference on Decision and Control*, IEEE, Piscataway, NJ, 2004, pp. 273–277.

[6] Lovera, M., and Astolfi, A., "Global Magnetic Attitude Control of Spacecraft in the Presence of Gravity Gradient," *IEEE Transactions on Aerospace and Electronic Systems*, Vol. 42, No. 3, July 2006, pp. 796–805.

[7] Leonard, B. S., "NPSAT1 Magnetic Attitude Control System," *Proceedings of the 16th Annual AIAA/USU Conference on Small Satellites*, Small Satellite Conference Services, Logan, UT, Aug. 2002, pp. 1–7; also Paper SSC02-V-7.

[8] Hughes, P. C., *Spacecraft Attitude Dynamics*, Dover Publication, New York, 2004, pp. 281–353.

[9] Chobotov, V. A., *Spacecraft Attitude Dynamics and Control*, Krieger, Malabar, FL, 1991, pp. 91–104.

[10] Baker, R. M., "Librations on a Slightly Elliptic Orbit," *ARS Journal*, Vol. 30, No. 1, Jan. 1960, pp. 124–126.

[11] Busch, R., and Flugge-Lotz, I., "Attitude Control of Stable and Unstable Satellites in an Elliptic Orbit," *Journal of Spacecraft and Rockets*, Vol. 6, No. 6, June 1969, pp. 685–691.

[12] Boykon, W., and Flugge-Lotz, I., "Attitude Control of a Satellite in an Elliptic Orbit," *Journal of Spacecraft and Rockets*, Vol. 4, No. 4, April 1967, pp. 436–442.

[13] Sorensen, J. A., "A Magnetic Attitude Control System for an Axisymmetric Spinning Spacecraft," *Journal of Spacecraft and Rockets*, Vol. 8, No. 5, May 1971, pp. 441–448.

[14] Schmidt, G. E., "The Application of Magnetic Attitude Control to a Momentum Biased Synchronous Communications Satellite," AIAA Paper 75-1055, 1975.

[15] Stickler, A. C., and Alfriend, K. T., "Elementary Magnetic Attitude Control System," *Journal of Spacecraft and Rockets*, Vol. 13, No. 5, May 1976, pp. 282–287.

[16] Elnagar, J., Kazemi, M. A., and Razzaghi, M., "The Pseudospectral Legendre Method for Discretizing Optimal Control Problem," *IEEE Transactions on Automatic Control*, Vol. 40, No. 10, 1995, pp. 1793–1796.

[17] Ross, I. M., and Fahroo, F., "Legendre Pseudospectral Approximations of Optimal Control Problems," *Lecture Notes in Control and Information Science 295*, edited by W. Kang, C. Borges, and M. Xiao, Springer–Verlag, New York, 2003, pp. 327–342.

[18] Ross, I. M., and Fahroo, F., "Pseudospectral Methods for Optimal Motion Planning of Differentially Flat Systems," *IEEE Transactions on Automatic Control*, Vol. 49, No. 8, Aug. 2004, pp. 1410–1413.

[19] Elnagar, J., and Razzaghi, M., "A Collocation-Type Method for Linear Quadratic Optimal Control Problems," *Optimal Control Applications and Methods*, Vol. 18, No. 3, 1997, pp. 1267–1272.

[20] He, S., and Unbehauen, R., "Pseudospectral Technique for Continuation Methods with Application to Nonlinear Control Problems," *IEEE Proceedings, Control Theory and Applications*, Vol. 151, No. 5, Sept. 2004, pp. 531–538.

[21] Williams, P., Blanksby, C., and Trivailo, P., "Receding Horizon Control of Tether System Using Quasilinearisation and Chebyshev Pseudospectral Approximations," AAS Paper 03-535, Aug. 2003.

[22] Williams, P., "Guidance and Control of Tethered Satellite Systems Using Pseudospectral Methods," AAS Paper 04-169, Feb. 2004.

[23] Yan, H., Fahroo, F., and Ross, I. M., "Optimal Feedback Control Laws by Pseudospectral Approximations," *Proceedings of the 2001 American Control Conference*, Vol. 3, IEEE, Piscataway, NJ, June 2001, pp. 2388–2393.

[24] Lu, P., "Close Form Control Laws for Linear Time-Varying Systems," *IEEE Transactions on Automatic Control*, Vol. 45, No. 3, 2000, pp. 537–542.

[25] Wertz, J. R. (ed.), *Spacecraft Attitude Determination and Control*, D. Reidel, Boston, 1978, pp. 779–786.

[26] Schaub, H., and Junkins, J. L., *Analytical Mechanics of Space Systems*, AIAA Education Series, AIAA, Reston, VA, 2003, pp. 160–170.

[27] Arduini, C., and Baiocco, P., "Active Magnetic Damping Attitude Control for Gravity Gradient Stabilized Spacecraft," *Journal of Guidance, Control, and Dynamics*, Vol. 20, No. 1, 1997, pp. 117–122.

[28] Kwon, W. H., and Pearson, A. E., "A Modified Quadratic Cost Problem and Feedback Stabilization of a Linear Systems," *IEEE Transactions on Automatic Control*, Vol. 22, No. 5, 1977, pp. 838–842.

[29] Mayne, D. Q., Rawlings, J. B., Rao, C. V., and Scokaert, P. O. M., "Constrained Model Predictive Control: Stability and Optimality," *Automatica*, Vol. 36, No. 6, 2000, pp. 789–814.

[30] Gong, Q., Kang, W., and Ross, I. M., "A Pseudospectral Method for the Optimal Control of Constrained Feedback Linearizable Systems," *IEEE Transactions on Automatic Control*, Vol. 51, No. 7, July 2006, pp. 1115–1129.

[31] Yan, H., and Alfriend, K. T., "Three-Axis Magnetic Attitude Control Using Pseudospectral Control Law in Eccentric Orbits," AAS Paper 06-103, Jan. 2006.

[32] Yan, H., Ross, I. M., and Alfriend, K. T., "Three-Axis Magnetic Attitude Control Using Pseudospectral Control Law," AAS Paper 05-417, Aug. 2005.

[33] Yan, H., Fleming, A., Ross, I. M., and Alfriend, K. T., "Real-Time Computation of Time-Optimal Magnetic Attitude Control," AAS Paper 05-233, Jan. 2005.